Nuclear Inst. and Methods in Physics Research, A 1031 (2022) 166514

Contents lists available at ScienceDirect

Nuclear Inst. and Methods in Physics Research, A

journal homepage: www.elsevier.com/locate/nima

Measurement of the muon flux in the bunker of Monte Soratte with the CRC detector

A. Candela [a], A. Cocco [a], N. D'Ambrosio [a], M. De Deo [a], A. De Iulis [c], M. D'Incecco [a], P. Garcia Abia [d], C. Gustavino [b,*], G. Gustavino [e], M. Messina [a], G. Paolucci [c], S. Parlati [a], N. Rossi [a]

[a] Laboratori Nazionali del Gran Sasso, Assergi (AQ), Italy
[b] Istituto Nazionale di Fisica Nucleare, Sezione di Roma, Italy
[c] Museo Percorso della Memoria, Sant'Oreste (RM), Italy
[d] CIEMAT, Centro de Investigaciones Energéticas, Medioambientales y Tecnológicas, Madrid, Spain
[e] Homer L. Dodge Department of Physics and Astronomy, University of Oklahoma, Norman OK, USA

ARTICLE INFO

Keywords:
Muon flux
Underground laboratory
Muon tomography
Muon radiography

ABSTRACT

In the context of the Ptolemy project, the need for a site with a rather low cosmogenic induced background led us to measure the differential muon flux inside the bunker of Monte Soratte, located about 50 km north of Rome (Italy). The measurement was performed with the Cosmic Ray Cube (CRC), a portable tracking device. The simple operation of CRC was crucial to finalize the measurement, as it was carried out in a site devoid of scientific equipment and during the COVID-19 lockdown. The muon flux measured at the Soratte hypogeum is about two orders of magnitude lower than the flux observed on the surface, suggesting the use of the Soratte bunker for hosting astroparticle physics experiments in which a low environmental background is required.

Introduction

The Ptolemy project aims at the detection of cosmic neutrino background (CNB) [1–3] produced in the early universe according to the Big Bang theory [4]. The extremely low reaction yield expected in this experiment suggests its installation in a underground site, to reduce the cosmic-ray induced background. In this concern, a preliminary study by the Ptolemy collaboration shows that a muon flux lower than about 1 m^{-2} s^{-1} sr^{-1} is adequate to prevent possible bias due to cosmic induced background which might hamper the performance of the experiment.

A candidate site to host the Ptolemy experiment is the bunker of the Soratte mountain, about 50 km north of Rome, Italy. Its construction started in 1937 as an air-raid shelter. During the 1967–1972 period its structure was modified to realize an antinuclear bunker. Presently, the bunker is composed of a network of tunnels and halls for a total length of about 4 km and it hosts the "Path of memory" historical museum [5]. The intensity of muons flux in the Soratte bunker is expected to be significantly lower with respect to the one at sea level, that is of the order of 70 m^{-2} s^{-1} sr^{-1} muons with momentum above 1 GeV/c (see for example [6,7] and references therein). The muon flux measurement discussed in this paper has been performed in the "War Room" of the museum with the Cosmic Ray Cube (CRC), a novel detector made mainly for educational purposes.

The paper is organized as follows: Section 1 describes the CRC detector, the detector performance and the event reconstruction are discussed in Section 2, Section 3 presents the data analysis and the results.

1. The CRC detector

The CRC detector is the evolution of the hodoscope exhibited in L'Aquila in 2009 during the Group of Eight (G8) summit meeting and afterwards installed in the Museum of Science (Teramo, Italy). That device consisted of 10 planes of Glass Resistive Plate Chamber (GRPC) equipped with orthogonal read-out strips. Its peculiar feature was the ability to visualize the cosmic-ray tracks with light-emitting diodes (LEDs) connected to the front-end electronics [8]. A more recent version of a visual hodoscope for cosmic rays is installed in the subway station "Toledo" (Naples, Italy) and other sites [9]. The most relevant improvement of this device is the use of scintillating bars coupled to silicon photomultipliers (SiPM) instead of GRPC detectors, making the device more suitable for outreach purposes. The CRC is a simplified version of the previous hodoscopes. It is a portable device, easy to construct and its operation requires only the standard electrical power.

The CRC is based on the use of STYRON 663 scintillating bars arranged as shown in Fig. 1. The bars are 24 cm long with a rectangular section of 4×1 cm^2. They are coated with Titanium dioxide (TiO_2), which reflects the scintillation light and prevents environmental light from entering inside the bars [10]. A wavelength shifting (WLS) fiber

* Corresponding author.
E-mail address: carlo.gustavino@roma1.infn.it (C. Gustavino).

https://doi.org/10.1016/j.nima.2022.166514
Received 2 November 2021; Received in revised form 19 January 2022; Accepted 9 February 2022
Available online 4 March 2022
0168-9002/

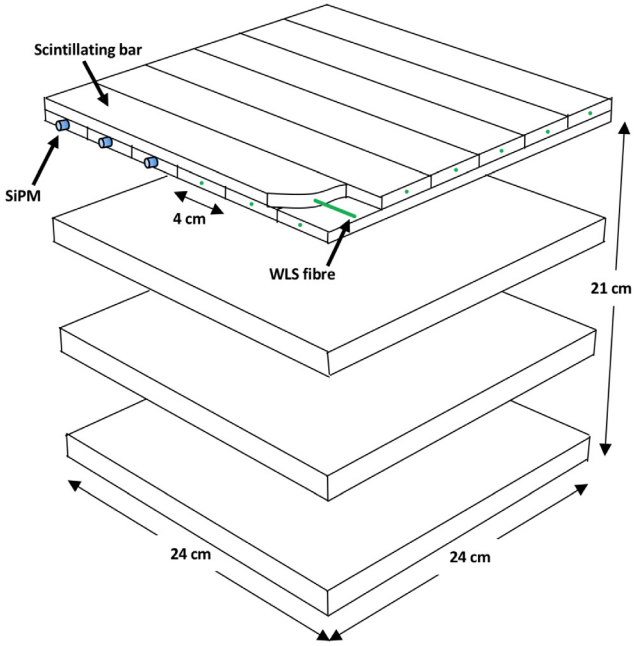

Fig. 1. Schematic drawing of the CRC detector.

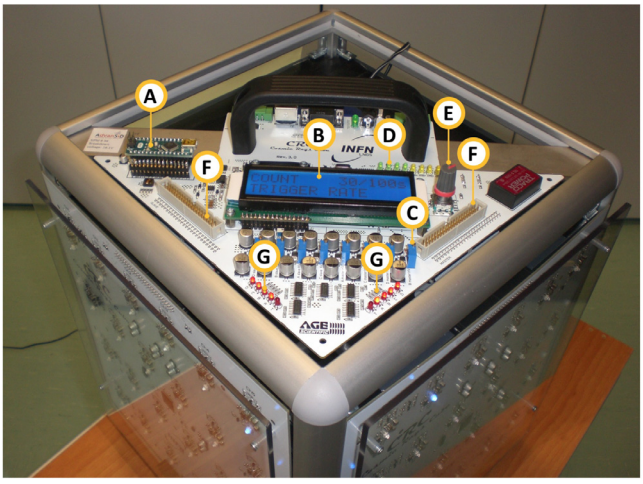

Fig. 2. CRC controller board. Arduino based trigger acoustic alert (A), display of set function (B), SiPM Bias voltage adjustment (C), trigger configuration LEDs (D), encoder to select menu function and value of selected parameters (E), voltage and signal probes (F), x counting rate LEDs (G).

Kuraray Y-11(200) with a diameter of 2 mm is inserted without gluing in each bar. The fiber collects and transmits the scintillation light to a silicon photomultiplier (SiPM) AdvanSiD ASD-RGB1C-M faced to one end of the fiber and converts photons into an electrical signal. The SiPMs have a sensitive area of 1.13 mm^2 and operate with a bias voltage of 32 V [11]. The real-time visualization of cosmic rays is provided by a set of LEDs, each one placed in correspondence of a SiPM. In total, the CRC is composed of four x-planes and four y-planes, each one consisting of 6 bars, for a total of 48 electronic channels. The detector is equipped with three printed circuit boards (PCB), two of which are implemented with an Altera Max V Complex Programmable Logic Device (CPLD) for signal processing. The third card unit (CONTROLLER) allows the setting of the signal thresholds, the SiPM bias voltages and the trigger configuration. In addition, it manages the data and provides the power supply to operate the CRC. The on board display and the encoder allow to define different functions such as the trigger configuration and the

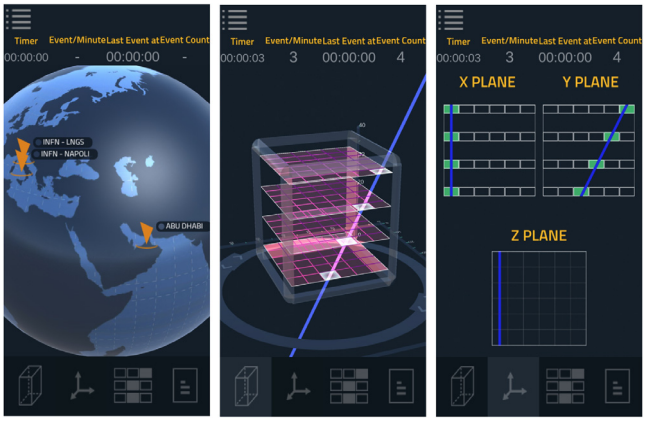

Fig. 3. Screenshots of the "Cosmic Ray Live" application for smartphones. From left to right: worldwide locations of CRC sites, 3D track reconstruction, projections of a muon track.

monitoring of channel rates (Fig. 2). A microchip controller is used to manage the digital pattern of events, that can be registered in a file together with their trigger time. The data files and several real-time functions, such as the event display, are available using a dedicated smartphone application ("Cosmic Ray Live") developed for both Android and iOS systems (Fig. 3). This application enables the connection of several CRCs around the world, providing a global network for educational purposes. Presently, CRCs are located at: Gran Sasso National Laboratory (Italy), New York University of Abu Dhabi (UAE) [12,13], INFN Sezione of Naples (Italy), and Canfranc Underground Laboratory (Spain).

In summary, the CRC detector has been conceived for educational purposes, with the aim of involving secondary school students in its construction and operation. In this concern, its design was addressed to realize a device easy to assemble and with an affordable cost. It is shown that the detector with a basic characterization allowed performing the muon flux measurement in the Soratte bunker.

2. Event reconstruction and data analysis

The 3-dimensional trajectories of muons crossing the detector are reconstructed from the 2-dimensional projections of the signals registered on the x and y views identified as the right and the left panels of the CRC detector (Fig. 4). The direction of each track is identified by the slope of the projected straight line in each view (Fig. 5), determined with a linear regression algorithm based on the least squares method. Each point is plotted in the figure with its standard deviation set to $1/\sqrt{12}$ of the strip width (based on the uniform distribution hypothesis).

Good events are defined by the following selection criteria:

1. each of the four planes of a lateral view has at least one LED turned on;
2. if two LEDs are turned on in a plane, they must be contiguous;
3. the reduced χ^2 of the linear regression must be lower than 1.5;
4. the conditions 1, 2 and 3 must be simultaneously valid for both the x and y views.

The first two conditions ensure that the event can be safely associated with a clean muon track, without sparse hits due to ambient radioactivity and/or electronic noise. Condition 3, suitably tuned with a Monte Carlo simulation, selects events produced by an ionizing particle moving along a straight trajectory. Finally, the last condition requires that both CRC views identify a clean track, allowing the reconstruction of its 3-dimensional direction.

The two angles θ_x and θ_y are defined between the reconstructed track and the z axis for each view (Fig. 5). The domain of both θ_x

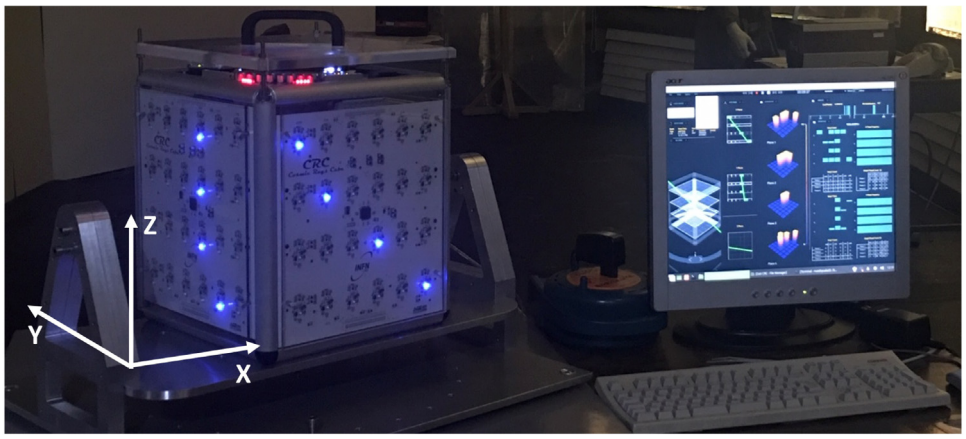

Fig. 4. Photograph of the CRC detector operating in the "War Room" of the underground "Path of memory" museum. A 3D track reconstruction of a muon crossing the hodoscope is well visible. The mechanical structure supporting the detector allows the rotation of the cube axis with respect to the zenith and azimuth angles.

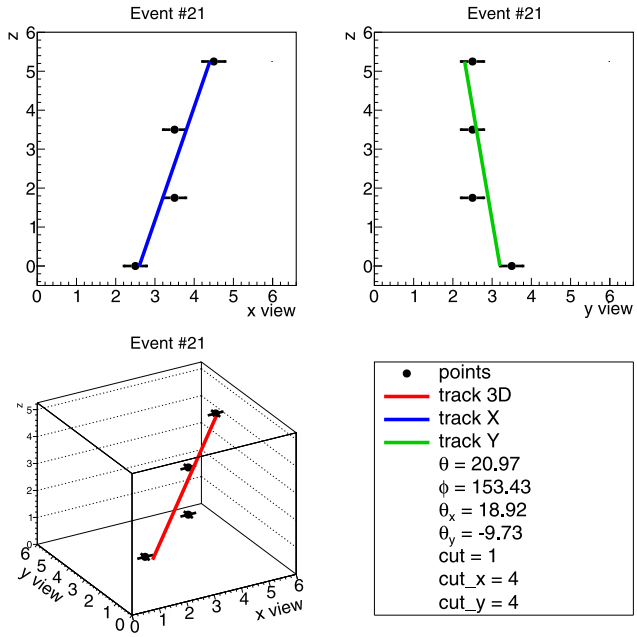

Fig. 5. Example of event reconstruction. *Top left and right*: reconstruction of the projections on the x and y views respectively. *Bottom left*: 3D reconstruction of the muon track in the CRC detector. *Bottom right*: legend with angles of interest and information about the event selection (all four layers have a fired strip in both CRC views).

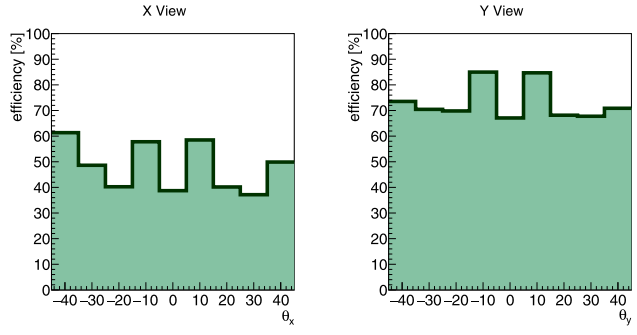

Fig. 6. Efficiency for x and y views. The efficiency is reported in percentage as a function of the view angles θ_x and θ_y in 9 bins of 10° width in the interval (−45°, -45°). The shapes of the efficiency distributions reflect the preferred trajectories resulting from the segmented structure of the detector. The statistical uncertainty on the efficiency is of the order of 0.1% and cannot be appreciated in the graph.

and θ_y is the fiducial angular interval [−45°, 45°]. This range is close to the maximal angular acceptance determined by the cubic shape of the detector and by the selection criteria, requiring all the four planes of each view to be crossed by the particle. The entire angular range is divided into 9 bins of 10° width. Hence, tracks populate 9 × 9 bins corresponding to 81 different directions with respect to the z axis of the CRC detector. This provides a smooth view of the event angular distributions which match approximately the intrinsic angular resolution given by the width of the bars.

The geometrical acceptance, in terms of the θ_x and θ_y angles, is given by the product of the projected acceptances in the x and y views:

$$A(\theta_x, \theta_y) = A(\theta_x)A(\theta_y). \tag{1}$$

The acceptance of both views $A(\theta_{x,y})$ only depends on the CRC geometry and on the adopted event selection, in which the four planes in each view are crossed by the particle. It can be expressed by the following formula:

$$A(\theta_{x,y}) = \cos\theta_{x,y}\left(1 - \frac{Z_0}{L_0}\tan|\theta_{x,y}|\right), \tag{2}$$

where $L_0 = 24$ cm and $Z_0 = 21$ cm are the width and height of the CRC, respectively (Fig. 1). For the events fulfilling the selection criteria, the total efficiency is the product of the efficiencies of the 4 planes, both in the x and y views.

The efficiency of each CRC plane was measured as a function of the track slope. About 10^6 muon events where used, providing a statistical error below 1% for each angular bin. The measured efficiency of a single plane properly working was about 93%. This value mainly depends on the light yield of the STYRON 663 scintillator, on the detector design and on the SiPM characteristics. The efficiency of the n_x-th plane of the x view with a given θ_x direction is defined as

$$\epsilon(n_x, \theta_x) = N(n_x, \theta_x)/N_{tot}(n_x, \theta_x), \tag{3}$$

where $N(n_x, \theta_x)$ is the number of events that fulfill the selection criteria for both views and belong to the θ_x angular bin, while $N_{tot}(n_x, \theta_x)$ also includes the events in which the n_x-th plane is inefficient (no LED on). The resulting efficiencies for the x and y $\epsilon(\theta_x)$ and $\epsilon(\theta_y)$, are depicted in Fig. 6. The y view efficiency is at the 75% level, as a result of the average plane efficiency of about 93% and the 4-fold coincidence requirement. The x view efficiency is about 50% mainly because of the presence of a channel which did not work throughout all measurements. The logical AND between the two views led to a CRC efficiency for each solid angle bin $\epsilon(\theta_x, \theta_y) = \epsilon(\theta_x)\epsilon(\theta_y)$ of typically 35%. As stated above, this overall efficiency is affected by the stringent requirements adopted to select events of optimal quality. The resulting

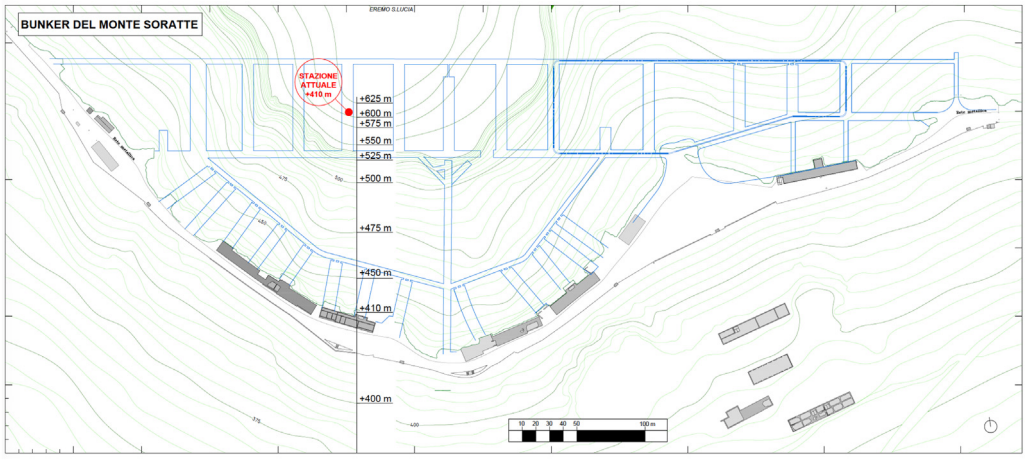

Fig. 7. Planimetry of the Soratte bunker overlapped to the level contour lines of Mt. Soratte. The red dot indicates the position of the CRC detector inside the "War Room" of the museum.

event rate made possible the measurement in the Soratte bunker in an integrated data taking time of about 2 months.

The differential muon flux is given by the following formula:

$$\Phi_\mu(\theta_x, \theta_y) = \frac{\mathcal{R}_{exp}}{\omega \cdot S \cdot A(\theta_{x,y})\epsilon(\theta_x, \theta_y)}, \tag{4}$$

where $\Phi_\mu(\theta_x, \theta_y)$ is the differential muon flux relative to the angular bin related to a specific direction (θ_x, θ_y), expressed in muons/s/sr; $\mathcal{R}_{exp}$ is the muon rate relative to the angular bin; ω is the solid angle defined in a bin (equal to 0.0305 sr for our $\Delta\theta_x = \Delta\theta_y$ bin size); $S = L_0^2 = 575\ cm^2$ is the surface of a CRC plane; $A(\theta_{x,y})$ and $\epsilon(\theta_x, \theta_y)$ are the detector acceptance and efficiency previously defined.

3. Muon flux in the soratte bunker

During the measurements, the detector was placed on a dedicated mechanical structure (see Fig. 4) able to rotate the detector with respect to the z and x axes in angular steps of $\Delta\phi = 15°$ and $\Delta\theta = 15°$ (θ and ϕ are the zenith the azimuth angles, respectively). In this way, it was possible to overcome the limited angular acceptance of CRC (of about 45° with respect to its z axis) in order to measure the differential muon flux in the whole upper hemisphere. To account for the CRC orientation, it is convenient to express the direction of the tracks in terms of standard polar angles, performing a change of variables and a proper trigonometrical rotation. In the following, terrestrial coordinates will be adopted, translating $\Phi_\mu(\theta_x, \theta_y)$ into $\Phi_\mu(\theta, \phi)$. The underground measurements were performed using the following 43 orientations (angles in degrees):

(i) $\theta = 0,\ \phi = 0, 45, 180$;
(ii) $\theta = 15,\ \phi = 0, 45, 90, \ldots, 315$;
(iii) $\theta = 30,\ \phi = 0, 45, 90, \ldots, 315$;
(iv) $\theta = 45,\ \phi = 0, 15, 30, \ldots, 345$.

Fig. 7 shows the planimetry of the Soratte bunker and the position of the detector used to measure the differential muon flux. It is located close to the south of the Soratte peak, at about 410 meters a.s.l. and covered by about 200 meters of rock along the vertical direction.

The first polar plot in Fig. 8 presents the differential muon flux of the upper hemisphere. The plot center ($\theta = 0°$) indicates the vertical direction, while the external circle corresponds to the horizon ($\theta = 90°$). As expected, the differential muon flux is not homogeneous and reflects the side CRC positioning relative to the Soratte peak. The highest flux measured is close to the horizon and it comes from the southern sector, as expected. Instead, the horizontal muon flux corresponding to an azimuthal angle of about $\phi = 338°$ (clockwise relative to the north) is lower, as only muons with very high energy can cross more than 1 km of rock present along this direction. A relatively low muon flux is also measured in the same ϕ at smaller zenith angles. This behavior can be easily explained by inspecting Fig. 9, which shows that the mountain ridge is just along this azimuthal direction. The overall anticorrelation of the differential muon flux with respect to the traversed rock thickness is well visible comparing the two polar plots of

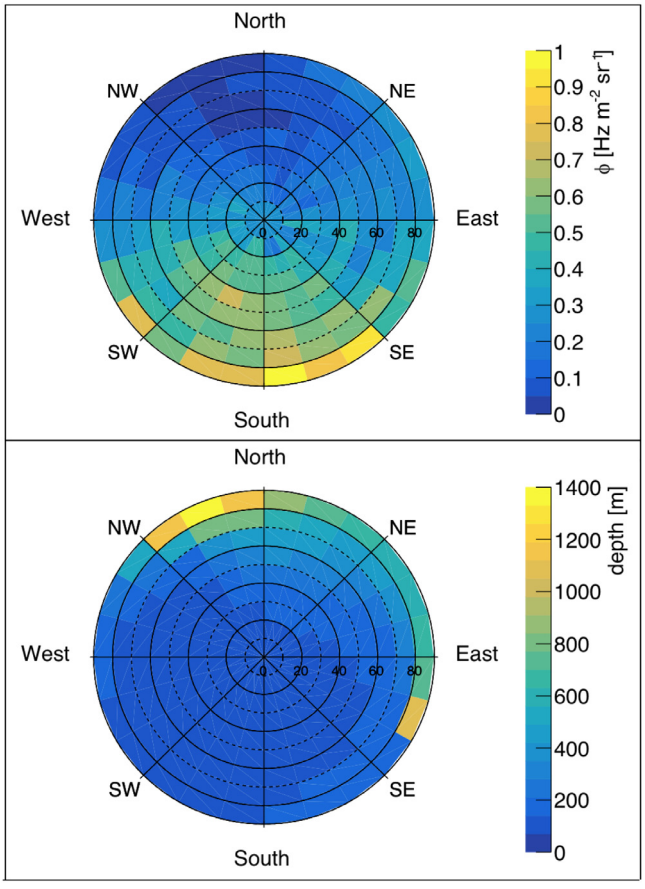

Fig. 8. Top: Polar plot of the differential muon flux as measured in the "War Room" of the Soratte bunker; bottom: slant depth of the Soratte mountain from the point of view of the CRC detector. The anticorrelation between the muon flux and the nominal thickness of rock crossed by the detected muons is well visible.

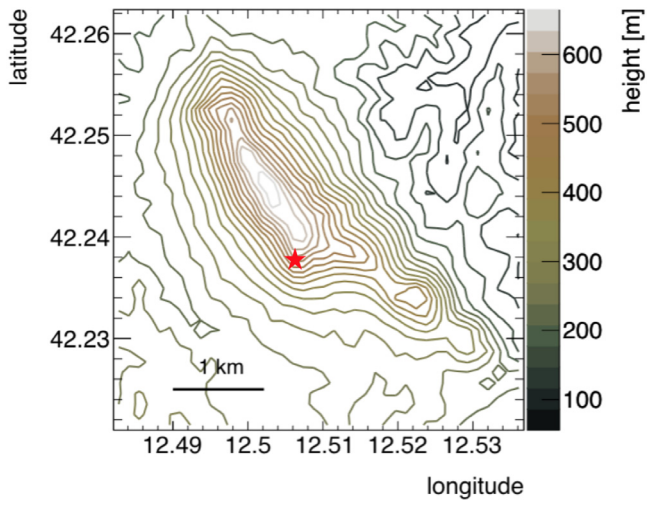

Fig. 9. Topographic profile of Monte Soratte. The red star indicates the position of the detector.

Fig. 8. On the bottom, the nominal rock thickness is shown (the tunnels and halls of the Soratte bunker shown in Fig. 7 are neglected in this plot): as expected, the higher the rock thickness, the lower the muon flux. The total averaged muons flux is $\Phi_\mu = 0.3\ \mathrm{m}^{-2}\ \mathrm{s}^{-1}\ \mathrm{sr}^{-1}$, more than 2 orders of magnitude lower than the typical flux measured on the surface [6,7].

4. Conclusions

The reported measurement is the first of a campaign aimed at searching for a site to eventually host long-standing astroparticle physics experiments such as PTOLEMY or other astroparticle physics experiments requiring a low cosmic ray induced background. The CRC detector proved to be very well suited for the measurement discussed in this paper, as it can be remotely controlled and does not require a special and complex equipment. These features were essential in the data taking performed during the COVID-19 pandemic lockdown period. Given the present results, we are planning to add the Soratte bunker to the educational CRC network at disposal of high school students. Thanks to the dedicated mechanical structure for vertical and horizontal rotation, it was possible to exploit the CRC features for a fine scanning of the differential muon rate, able to highlight the details of the mountain above the bunker. The total underground muon rate is found to be compatible with two orders of magnitude attenuation as expected from the average thickness of the rock.

CRediT authorship contribution statement

A. Candela: Conceptualization, Resources, Software. **A. Cocco:** Funding acquisition. **N. D'Ambrosio:** Funding acquisition. **M. De Deo:** Conceptualization, Resources, Software. **A. De Iulis:** Validation, Data curation. **M. D'Incecco:** Conceptualization, Resources, Software. **P. Garcia Abia:** Formal Analysis, Writing and review original draft. **C. Gustavino:** Conceptualization, Resources, Software, Formal analysis, Writing and review original draft. **G. Gustavino:** Formal analysis, Writing and review original draft. **M. Messina:** Formal analysis, Writing and review original draft, Project administration. **G. Paolucci:** Data curation, Resources. **S. Parlati:** Sotware, Resources. **N. Rossi:** Conceptualization, Resources, Software, Formal analysis, Writing and review original draft.

Declaration of competing interest

The authors declare that they have no known competing financial interests or personal relationships that could have appeared to influence the work reported in this paper.

Acknowledgments

We acknowledge the invaluable contribution of the mechanical workshop at LNGS. Also, we thank the staff of the "Path of Memory" museum for the warm hospitality and for helping with the installation and the operation of the detector. Finally, we thank Adriano Di Giovanni who helped with the proofreading. This work has been funded by INFN.

References

[1] The Ptolemy Collaboration, E. Baracchini, et al., [physics.ins-det].
[2] The Ptolemy Collaboration, M.G. Betti, et al., J. Cosmol. Astropart. Phys. 07 (2019) 047.
[3] The Ptolemy Collaboration, M.G. Betti, et al., Prog. Part. Nucl. Phys. 106 (2019) 120–131.
[4] S. Weinberg, Phys. Rev. 128 (1962) 1457, http://dx.doi.org/10.1103/PhysRev.128.1457.
[5] G. Paolucci, G. Lo Gaglio, in: Bunker Soratte (Ed.), Il Bunker Del Soratte - Una Montagna Di Storia, 2018, Sant'Oreste (Roma), http://www.bunkersoratte.it.
[6] P.A. Zyla, et al., The review of particle physics (particle data group), Prog. Theor. Exp. Phys. 2020 (2020) 083C01, 2020.
[7] P.K.F. Grieder, Cosmic Rays at Earth, Elsevier Science, 2001.
[8] R. Antolini, et al., Radiat. Meas. 44 (9–10) (2009) 926–928.
[9] R. Antolini, et al., NIM-A 824 (2016) 190–191.
[10] A. Pla-Dalmau, A.D. Bross, K.L. Mellott, NIM-A 466 (2001) 482–491.
[11] AdvanSiD ASD-RGB1C-M SiPM data sheet, https://advansid.com/attachment/get/up_61_1432732739.pdf.
[12] A. Mannaei, et al., JINST 13 (2018) T07001.
[13] F. Arneodo, et al., NIM-A 936 (2019) 242–243.